THE JOURNAL OF PHYSICAL CHEMISTRY B

 VOLUME 107, NUMBER 19, MAY 15, 2003

ARTICLES

Controlled Opening of Single-Wall Carbon Nanohorns by Heat Treatment in Carbon Dioxide

Elena Bekyarova,[†] Katsumi Kaneko,[*,‡,§] Masako Yudasaka,[†] Daisuke Kasuya,[||] Sumio Iijima,[†,||,⊥] Ana Huidobro,[#] and Francisco Rodriguez-Reinoso[#]

JCORP-JST, c/o NEC Corporation, 34 Miyukigaoka, Tsukuba 305-8501, Japan, Department of Chemistry, Faculty of Science, Chiba University, 1-33 Yayoi, Inage, Chiba 263, Japan, Center for Frontier Electronics and Photonics, Chiba University, 1-33 Yayoi, Inage, Chiba 263, Japan, Meijo University, 1-501 Shiogamaguchi, Tempaku, Nagoya 468-8502, Japan, NEC Corporation, 34 Miyukigaoka, Tsukuba 305-8501, Japan, and Departamento de Quimica Inorganica, Universidad de Alicante, Apartado 99, E-03080, Alicante, Spain

Received: August 11, 2002; In Final Form: February 19, 2003

The opening of *bud*-type single-wall carbon nanohorns (SWNHs) by heat treatment in CO_2 was studied by TEM and nitrogen adsorption (77 K). The adsorption isotherms indicate that oxidation by CO_2 at 1273 K provides a sufficient nanohorn opening. The pore structure parameters of the open nanohorns can be controlled by varying the treatment conditions; the size of the generated nanopores increases with the temperature and time of treatment. In addition, TPD experiments indicate a significant decrease of the oxygen content in SWNHs opened by heat treatment in CO_2. This is in contrast to the procedures reported in the literature for opening of carbon nanotubular structures, typically introducing oxygen functional groups.

1. Introduction

The opening of carbon nanotubes (CNTs) is an issue of interest from both fundamental and experimental standpoints. The unique structure of CNTs offers possibility for nanoconfinement of molecular species in the tubular cavity.[1−4] Additionally, the internal space of the nanotubes holds a great potential for adsorption utilization.[5,6] Since the growth process of CNTs energetically favors a closed structure, nanotube opening with little loss of material and controlled functionalization is desired. Several techniques have been applied for opening of CNTs. Among them are heat treatment in O_2,[7,8] air,[9] O_3,[10] H_2O_2,[10] CO_2,[11] ultrasonication in $H_2SO_4HNO_3$ and H_2O_2/H_2SO_4,[12] reflux in HNO_3,[13] and chemical activation with KOH[14] and supercritical water.[15] Despite the extensive research on the nanotube opening, little is known about the mechanism and the factors controlling the opening process. As a result, carbon nanotubular materials with large surface area are scarcely reported.[16,17] Even purified open CNTs have surface area which is far from the predicted theoretical values. In this study, we address the opening of single-wall carbon nanohorns (SWNHs) by treatment in CO_2. SWNHs are attractive for adsorption utilization as they are easily produced in large quantities and with high purity.[18,19] We discuss the possibility of controlling the opening process by varying the treatment conditions. In addition to the development of the pore structure, the effect of the CO_2 treatment on the surface chemistry was studied. It is

* Corresponding author. Tel:+81-43-290-2779. Fax:+81-43-290-2788. E-mail: kaneko@pchem2.s.chiba-u.ac.jp.
† JCORP-JST, c/o NEC Corporation.
‡ Department of Chemistry, Faculty of Science, Chiba University.
§ Center for Frontier Electronics and Photonics, Chiba University.
|| Meijo University.
⊥ NEC Corporation.
Universidad de Alicante.

10.1021/jp026737n CCC: $25.00
Published on Web 04/22/2003

known that most of the techniques for nanotube opening introduce various oxygen functionalities at the open ends of the nanotubes. Oxygen groups alter the physicochemical properties of CNTs such as electrical, wettability, adsorption of polar molecules, and chemical reactivity. Our results show that the thermal treatment in CO_2 decreases significantly the oxygen content in the nanohorn structure. Thus, annealing in CO_2 atmosphere at elevated temperature might be an efficient approach to reduce the oxygen content in the structure of open-ended carbon nanotubular materials.

2. Experimental Section

bud-SWNHs (b-NH) used in this study are produced by CO_2 laser irradiation of graphite in He atmosphere at 760 Torr and room temperature.[18,19] The pristine b-NHs were heated in flowing CO_2 (50 mL min^{-1}) at 1173 and 1273 K for 1, 5, and 10 h, respectively. The material was cooled in CO_2 atmosphere. The samples are designated as b-NH-*x*/*y*, where *x* is the temperature in K and *y* is the time in hours at which the experiment was conducted.

TEM micrographs were obtained with a conventional transmission electron microscope (Topcon EM-002B) at 200 kV accelerating voltage.

The adsorption isotherms of N_2 were measured volumetrically at 77 K with an Autosorb-1 (Quantachrom). The samples were treated at 423 K and 10^{-4} Pa for 2 h prior to the adsorption measurements.

Temperature-programmed desorption (TPD) was carried out from 298 to 1273 K in flowing He (50 mL min^{-1}) and heating rate of 10 deg min^{-1}. All samples were handled in air before the TPD experiments. Thermogravimetric analysis (TGA) was conducted in CO_2 with gas flow rate of 30 mL min^{-1} and heating rate of 10 deg min^{-1}.

3. Results and Discussion

Graphitic structures have low reactivity toward CO_2. The reaction of graphite with CO_2 is known as the Boudouard reaction:

$$C(\text{graphite}) + CO_2 = 2CO$$

$$\Delta H_{298.15K} = 173.26 \text{ kJ mol}^{-1}; \Delta G_{1200K} = -39.41 \text{ kJ mol}^{-1}$$

The reaction is endothermic and in the absence of a catalyst it proceeds with a substantial rate at temperatures above 1123−1173 K.[20] SWNH consists of a graphene sheet rolled into a cylinder closed with horn-shaped caps. Hence, the reactivity of a carbon nanohorn is expected to be similar to that of graphite. Two simultaneous processes would take place upon heating of SWNHs at high temperature in CO_2 atmosphere. The first process is thermal decomposition and evolution of oxygen-containing groups present on the nanohorn walls. The oxygen functionalities found in carbon nanotubes[21−23] and other carbonaceous materials[24−26] are expected to exist in SWNHs. The second process is reaction between the nanohorns and CO_2, taking place predominantly at the caps and the topological and chemical defects in the carbon walls. Both processes open nanowindows on the nanohorn walls as illustrated schematically in Figure 1.

We examined the reactivity of SWNHs toward CO_2 by thermo-gravimetric analysis. Figure 2 shows the TG curve in CO_2 for pristine SWNHs. The curve does not exhibit clear weight loss steps, but it can be approximately divided into three regions. In the first region (below 473 K) the weight loss is

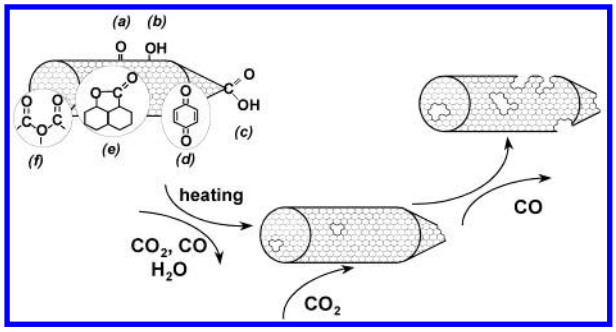

Figure 1. Schematic illustration of nanohorn opening during heat treatment in CO_2. For simplicity the present oxygen functional groups are drawn only on the untreated nanohorn: (a) carbonyl, (b) hydroxyl, (c) carboxyl, (d) quinone, (e) lactone, and (f) anhydride groups.

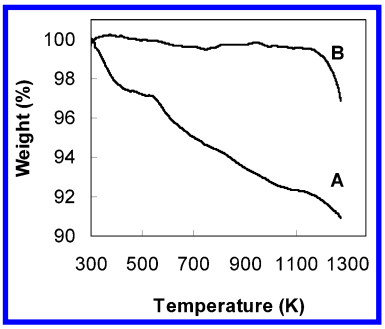

Figure 2. TGA of *bud*-SWNH (A) measured at 10 deg/min in flowing CO_2. TGA of graphite (B) measured at the same conditions is given for comparison.

associated with the evolution of physisorbed and weakly chemisorbed species, trapped in the pore structure of SWNHs. The next region, between 473 and 1073 K, corresponds to the thermal decomposition of oxygen functional groups present in the nanohorn structure. The TG curve of graphite (Figure 2, curve B) shows much less weight loss in these two regions. A slightly steeper decrease in the TG curve is observed above 1100 K, indicating a reaction between the nanohorns and CO_2. The total weight loss in the temperature range 298−1273 K is about 10%, showing a low reactivity of the nanohorns toward CO_2. Thus, the low reaction rate between CO_2 and SWNHs should allow an effective tuning of the nanohorn opening by varying the treatment conditions.

TEM observations did not show any significant changes in the morphology of the SWNH assemblies after heat treatment in CO_2. Representative images of the pristine and oxidized SWNHs are given in Figure 3. Since a direct observation of the nanowindows created in the carbon nanohorn walls by TEM is difficult, the opening of the nanohorns was studied experimentally with physical adsorption measurements. The tubular cavity of the nanohorn represents a nanopore with a diameter of 2 to 3 nm as observed by TEM. Theoretical calculations[27] show a very strong fluid−solid interaction potential in the internal cylindrical nanospace and consequently any opening of the nanohorns should affect significantly their adsorption behavior.

The nitrogen adsorption isotherms at 77 K are shown in Figure 4. After heat treatment in CO_2 at 1273 K, SWNHs show an enhanced adsorption capacity (Figure 4a), suggesting opening of the nanohorns. As discussed above, the treatment at high temperature is accompanied by evolution of oxygen groups from the carbon surface and this could result in eventual opening of the nanohorns. To distinguish between the opening of SWNHs caused by the evolution of the oxygen functional groups and the opening due to the reaction between CO_2 and carbon

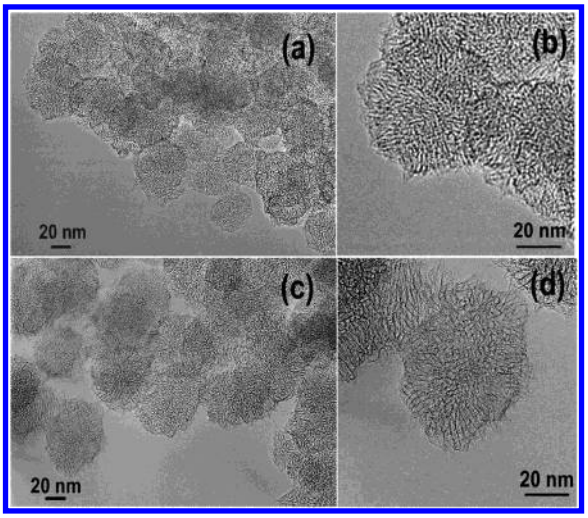

Figure 3. TEM images of *bud*-SWNHs: pristine (a and b) and treated in CO_2 at 1173 K for 5 h (c and d).

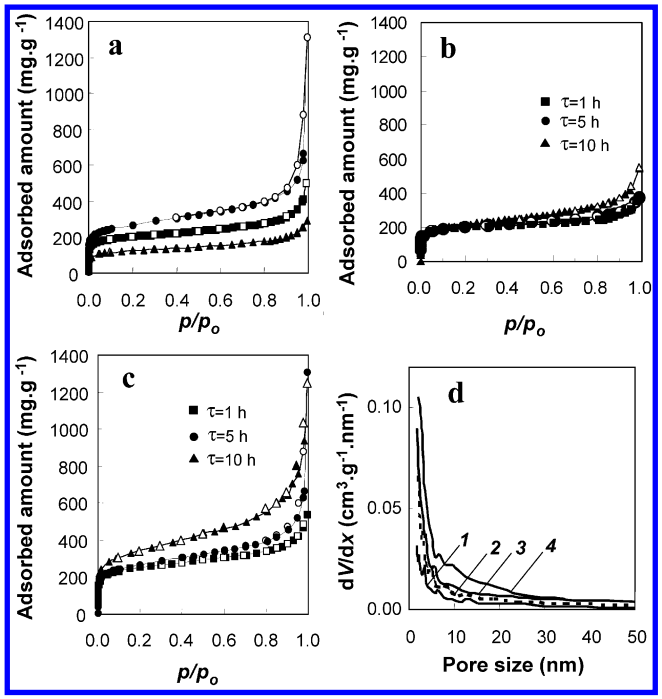

Figure 4. Nitrogen adsorption isotherms at 77 K and PSD curves of *bud*-SWNHs: (a) isotherms of pristine b-NH (▲) and SWNHs treated at 1273 K for 5 h in Ar (■) and CO_2 (●); (b) isotherms of *bud*-SWNHs treated in CO_2 at 1173 K for different time τ; (c) isotherms of *bud*-SWNHs heat treated in CO_2 at 1273 K for different time τ. Closed and open symbols denote adsorption and desorption, respectively; (d) mesopore size distribution curves of pristine b-NH (curve 1) and SWNHs treated in CO_2 at 1273 K, b-NH-1273/1 (curve 2), b-NH-1273/5 (curve 3), and b-NH-1273/10 (curve 4).

nanohorns, pristine SWNHs were heat treated in an inert atmosphere (Ar). The isotherm of the heated in Ar SWNHs exhibits a higher uptake compared with that of the pristine SWNHs (Figure 4a). However, the uptake of the isotherm is lower than that observed for the nanohorns treated in CO_2 at the same temperature and time (1275 K, 5 h). This confirms that reaction between the carbon nanohorns and CO_2 causes opening of the nanohorns. To study the effect of the treatment conditions on the adsorption properties of SWNHs, the nanohorn material was heated in flowing CO_2 at 1173 and 1273 K for different time. The nitrogen adsorption isotherms reveal that the adsorption capacity of the nanohorns heated at 1173 K is affected very little by the time of treatment (Figure 4b). A pronounced enhancement of the adsorption capacity with the time is achieved when the oxidation is carried out at 1273 K (Figure 4c). After treatment at 1273 K for 10 h a large number of SWNHs are open, due to the increased reaction rate with the temperature. Additionally, the isotherm of SWNHs heated for 10 h has a steeper slope, suggesting modification of the mesopore structure. This is confirmed by the mesopore size distribution curves obtained by the BJH (Barrett-Joyner-Hallenda) method and illustrated in Figure 4d. The pore size distribution (PSD) curve of b-NH-1273/10 shows an increased number of pores with size between 5 and 20 nm. Mesopores of size larger than 5 nm could be formed only between the spherical SWNHs assemblies. It is unlikely that the developed mesopores originate from separation between nanohorns in the assembly as such changes in the morphology would be registered by TEM. Consequently, the observed mesoscopic changes indicate an increase of the *inter*-assembly space. The assemblies have spherical shape with an average diameter of about 60−70 nm, as shown in Figure 3. Originally, the assemblies are attracted by van der Waals forces. As the reaction between nanohorns and CO_2 proceeds, the assemblies should separate and reorganize giving rise to changes in the mesopore size distribution.

To understand the changes in the pore structure after treatment at different conditions, the porosity parameters were evaluated by the subtracting pore effect (SPE) method for α_s-plot.[28] Analyzing the porosity, we considered a bimodal structure, which consists of *interstitial micropores* (formed between the individual nanohorns) and *internal* pores (originating from the internal cavities of the nanohorns). The internal nanopores become available for adsorption after opening of the nanohorns, i.e., after the CO_2 treatment. On the basis of the TEM observations, we assume that the oxidation opens the nanohorns without significantly altering their organization inside the assembly, i.e., the interstitial porosity. Consequently, the isotherm corresponding to the adsorption inside the open-ended nanohorns can be obtained from the isotherm of the oxidized SWNHs by subtracting the isotherm of the pristine SWNHs. The parameters of the internal and interstitial pore structures are evaluated by applying the SPE method to the subtracted isotherms, and the data are summarized in Table 1. The main parameters of the interstitial pore structure are the interstitial pore volume (V_{mi}^{intrst}) and pore width (w). The parameters characterizing the internal pore structure are the internal pore volume (V_{mi}^{in}) and pore diameter (d). The pore width and pore diameter are obtained as described elsewhere[29] from simple geometrical considerations assuming quasi slitlike and cylindrical models for the interstitial and internal pores, respectively. The data in Table 1 show that the specific surface area and the micropore volume increase with the temperature of treatment. Treatment at 1173 K does not result in a very large increase of the surface area and micropore volume of SWNHs even after treatment for 10 h. Apparently, only a few nanohorns open at this temperature. Treatment at 1273 K opens a larger number of nanohorns and, with increasing the time of treatment, both the surface area and micropore volume increase. An interesting observation from the adsorption analysis is that at both temperatures the diameter of the internal pores increases with the time of treatment. Such an increase of the diameter indicates an additional opening of nanohorns with a larger diameter. Consequently, nanohorns with smaller diameter should open first due to their higher reactivity. The diameter-dependent burning of other carbon nanotubular materials has been studied by Raman[30] and absorption spectroscopy.[31] The fact that nanohorns treated at 1173 K for different lengths of time have the same

TABLE 1: Pore Structure Parameters of *bud*-SWNHs[a]

sample	a_t ($m^2\ g^{-1}$)	a_{ext} ($m^2\ g^{-1}$)	V_t ($cm^3\ g^{-1}$)	V_{me} ($cm^3\ g^{-1}$)	V_{mi}^t ($cm^3\ g^{-1}$)	V_{mi}^{intrst} ($cm^3\ g^{-1}$)	w (nm)	V_{mi}^{in} ($cm^3\ g^{-1}$)	d (nm)
b-NH	320	100	0.32	0.21	0.11	0.11	1.0		
b-NH-1173/1	566	79	0.48	0.23	0.22	0.12	1.0	0.10	1.5
b-NH-1173/5	558	102	0.44	0.22	0.22	0.12	1.0	0.10	1.7
b-NH-1173/10	560	147	0.64	0.38	0.22	0.12	1.0	0.10	2.1
b-NH-1273/1	668	148	0.60	0.34	0.26	0.11	1.0	0.15	2.0
b-NH-1273/5	670	180	0.82	0.48	0.27	0.11	1.0	0.16	2.4
b-NH-1273/10	820	250	1.16	0.62	0.35	0.11	1.0	0.23	2.7
b-NH-1273/5(Ar)	546	135	0.51	0.31	0.20	0.11	1.0	0.08	1.7

[a] The total surface area (a_t) is calculated from the slope of the straight line passing through the origin of the α_s-plot; the external surface area (a_{ext}) is proportional to the slope of the linear branch at high α_s-region ($a = 2.08 \cdot$slope, where 2.08 is a constant related to the structure parameters of the standard used for constructing the α_s-plot); V_t is the total pore volume calculated from the uptake at $p/p_o = 0.98$; V_{me} is obtained from integrating the area under the PSD curves, since subtraction of V_t and V_{mi} overestimates the mesopore volume for the samples giving isotherms with steep increase at $p/p_o \rightarrow 1$; $w = 2V_{mi}^{intrst}/a_{mi}^{intrst}$; $d = 4\ V_{mi}^{in}/a_{mi}^{in}$, where a_{mi}^{in} and a_{mic}^{in} are the micropore surface areas ($a_{mic} = a_t - a_{ext}$) estimated from the corresponding subtracted isotherms.

micropore volume whereas the average diameter of the internal nanopores increases suggests that two simultaneous processes might take place: first, widening of the nanowindows on the nanohorn walls resulting in partial burning of the nanohorns, and second, opening of nanohorns with bigger diameter as the oxidation proceeds. It should be noted that at present there is no better method to separately analyze the interstitial and internal sub-structures, which consist of pores with different geometry. On the other hand, it cannot be excluded that the long oxidation process introduces changes in the interstitial pore structure such as cracks between adjacent nanohorns and partial burning of nanohorns. Although these changes are unlikely to greatly influence the results from the analysis, they would be examined at the next stage of the research. In summary, the adsorption analysis reveals a selective opening of nanohorns by treatment in CO_2, which can be controlled by changing the oxidation conditions. The conditions used in this study can be applied to generate open *bud*-SWNHs and the average diameter of the internal nanopores could be increased with increasing the time of treatment. In contrast, the average nanopore diameter of open SWNHs, obtained by heating b-NHs in oxygen, is not affected significantly by the treatment conditions.[29] Given the fast reaction between oxygen and graphene sheets, the opening of nanohorns should occur randomly at carbon sites with different reactivity and, therefore, the enhancement of the porosity with the temperature is accompanied with small changes in the diameter of the open nanohorns. On the other hand, our studies on porosity development in SWNHs by heating in O_2[29] and CO_2 show that the temperature of treatment is a very important factor for enhancement of the surface area and pore volume. However, the temperature for O_2 treatment is limited by the progressive burning of nanohorns and changes in the structure,[19] while the temperature for CO_2 treatment is restricted by possible coalescence of adjacent nanohorns and structural transformations.[32,33]

An alternative approach for development of porosity is successive treatment in O_2 and CO_2. The choice for heating in O_2 before treatment in CO_2 is based on the understanding of the mechanism of nanohorn opening. The treatment in oxygen produces many nanowindows with different size, generating at the same time defective sites in the form of oxygen impurities, vacancies, etc. A selective attack of the defective sites by CO_2 molecules would promote further opening of the nanohorns. In addition, as shown previously[29] some of the nanowindows created by heating in oxygen are very narrow and not permeable to nitrogen gas molecules. Heating in CO_2 will effectively widen such nanowindows. Figure 5 shows the nitrogen isotherm of b-NHs treated in O_2 at 693 K for 10 min followed by heating in CO_2 at 1173 K for 5 h. Obviously, the combined treatment

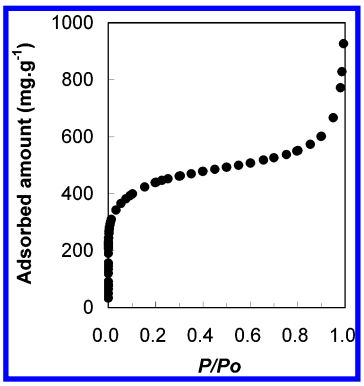

Figure 5. Nitrogen adsorption isotherm at 77 K of *bud*-SWNHs heated in oxygen at 693 K for 10 min followed by treatment in CO_2 at 1173 K for 5 h.

enhances significantly the adsorption capacity. The estimated surface area and micropore volume for this sample are 1070 $m^2\ g^{-1}$ and 0.50 $cm^3\ g^{-1}$, respectively.

The heat treatment in CO_2 is expected to affect the surface chemistry of carbon nanohorns. Usually, the oxidation process used for nanotube opening introduces various oxygen-containing species in the nanotube structure. Accordingly, opening of *dahlia*-SWNHs by heating in oxygen was found to increase the amount of the oxygen-containing groups more than 4 times in comparison with the pristine SWNHs.[34] Temperature-programmed desorption (TPD) experiments were performed to analyze the surface chemistry of SWNHs before and after the CO_2 treatment. The TPD analysis in this study is aimed at understanding the effect of the CO_2 treatment on the oxygen content in the structure of SWNHs. The data are compared with the pristine b-NH.

The TPD profiles of the CO_2-treated nanohorns were found difficult to interpret since they exhibit very broad features without well-resolved peaks, and a precise evaluation of the nature of the oxygen-containing groups, based solely on their thermal stability, is not straightforward. Further studies and techniques are necessary to understand the formation of oxygen functional groups in SWNHs during and after heating in CO_2. Figure 6 shows the TPD spectra of b-NH and the open SWNHs obtained by treatment in CO_2 at different conditions. An important observation is that the CO_2-treated nanohorns release less oxygen-containing decomposition products as compared to b-NH, indicating a decrease of the oxygen content in the carbon structure. This is in contrast to other techniques for opening of carbon nanotubular materials reported in the literature.[21,34,35] The activation of other carbon materials with CO_2 is also known to increase the amount of oxygen surface species.[36]

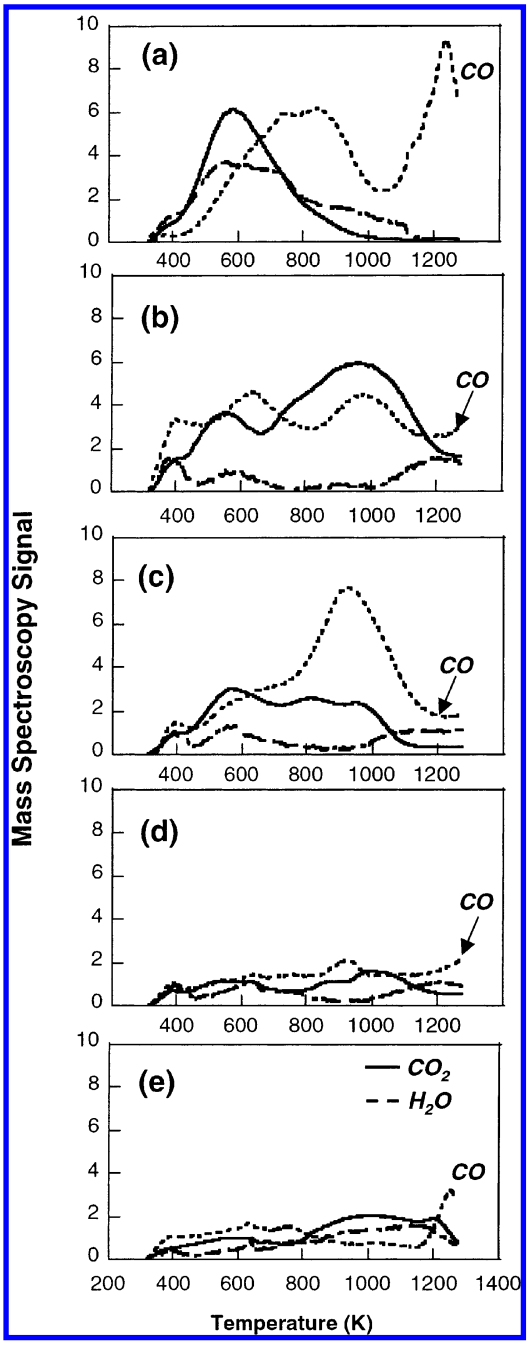

Figure 6. TPD spectra of (a) pristine b-NH, (b) b-NH-1173/1, (c) b-NH-1173/5, (d) b-NH-1273/1, (e) and b-NH-1273/5.

The pristine SWNHs (Figure 6a) desorb CO_2 and CO in a broad temperature range. CO_2 evolves as a prominent product at low temperature giving a broad peak with maximum at 600 K and a shoulder at around 780 K. Numerous studies on the nature of oxygen surface groups in carbonaceous materials unambiguously attribute the evolved CO_2 at low temperature (373−673 K) to the decomposition of carboxylic groups (see ref 37 and the references therein). CO_2 evolving at higher temperatures (673−923 K) is generally assigned to anhydride and lactones, both decomposing in the same temperature range.[37] The CO profile exhibits two broad peaks at 800 and 1225 K. The first peak appears to be a superposition of two or more peaks. The temperature range of the peak corresponds to the thermal stability of anhydride, phenol, and ether groups and respectively, such groups are expected to be present in the structure of b-NH. However, assignment of the peak to a specific group is difficult. The second peak is tentatively assigned to carbonyl and quinone groups.[38] Adsorption of O_2, CO_2, and H_2O on a clean graphite surface is known to form predominantly semiquinone groups decomposing upon heating at 973−1253 K.[38] As SWNHs are generated in an inert atmosphere (He), the oxygen groups observed in the TPD spectra are not formed during the synthesis process. However, exposed to air, the defects in the graphitic structure of SWNHs will readily adsorb O_2, CO_2, and H_2O, forming various oxygenated species.[38,39]

TABLE 2: Amounts of Evolved Gases from TPD Analysis and Oxygen Content for As-Grown and CO_2-Treated SWNHs

sample	CO_2 (mmol g^{-1})	CO (mmol g^{-1})	O/C %
b-NH	0.25	0.81	2.3
b-NH-1173/1	0.65	0.22	2.2
b-NH-1173/5	0.23	0.70	1.7
b-NH-1273/1	0.29	0.12	0.9
b-NH-1273/5	0.24	0.16	1.0

The samples treated in CO_2 at 1173 and 1273 K show very different CO and CO_2 profiles in comparison with b-NH. For all CO_2-treated samples there is a significant decrease of the CO-evolving groups, which almost diminish for the samples treated at 1273 K (b-NH-1273/1 and b-NH-1273/5). Usually, gas-phase oxidation increases significantly the presence of CO-precursor groups.[31,34] Additionally, the high-temperature CO peak observed at 1225 K for b-NHs does not appear in the CO_2-treated SWNHs. These groups are possibly removed as a result of the gasification reaction rather than thermal decomposition, because they are not observed in the TPD spectra of the samples treated at 1173 K, a temperature at which these groups are stable. The CO_2 profiles represent a broad continuum in the studied temperature range. As compared to b-NHs, there is a significant change in the ratio of low-thermal stability to high-thermal stability groups. There is a decrease of the low-temperature groups and a slight increase of the groups decomposing at high temperature (around 900 K). The continuous feature of the spectra (especially for the samples treated at 1273 K) is likely to originate from the same kind of species bound to different type of edge sites (zigzag, armchair, etc.) giving rise to a distribution in the activation energy of desorption. It is interesting to note that evolution of CO_2 was detected even at very high temperature (above 1000 K) for all samples. There is little information in the literature on CO_2-evolution at such high temperatures,[25,40] and the origin of the CO_2-precursor remains unexplained. The TPD spectra were measured with two different apparatus and showed very similar results.

The amounts of CO and CO_2 evolved from the samples were determined by integrating the area under the curves and the data are presented in Table 2. The O/C ratio in the samples is calculated from the evolved CO, CO_2, and H_2O including the physisorbed amounts, which cannot be precisely evaluated from the TPD spectra. The data clearly show that the heat treatment in CO_2 at 1173 and 1273 K decreases the oxygen content in the obtained open SWNHs.

4. Conclusions

This study on the heat treatment of *bud*-SWNHs in CO_2 atmosphere has revealed a number of important facts related to the controlled opening of carbon nanotubular structures.

1. The opening of SWNHs by heating in CO_2 atmosphere can be controlled by varying the treatment conditions. The oxidation of b-NHs with CO_2 at 1273 K opens a sufficient number of nanohorns, whereas few nanohorns open at lower temperature. The average size of the generated nanopores

increases with the time of treatment. This is of significant importance considering the possible sieving effect application of carbon nanotube structures.

2. Heat treatment in CO_2 decreases the oxygen content in the structure of the generated open-SWNHs. Hence, heat treatment in CO_2 is an effective approach to obtain open nanohorns with a reduced oxygen content.

Acknowledgment. E.B. is grateful to the Japan Science and Technology Corporation (JST) for the STA fellowship.

References and Notes

(1) Ajayan, P. M.; Iijima, S. *Nature* **1993**, *361*, 333.
(2) Smith, B. W.; Monthioux, M.; Luzzi, D. E. *Nature* **1998**, *396*, 323.
(3) Hirahara, K.; Suenaga, K.; Bandow, S.; Kato, H.; Okazaki, T.; Shinohara, H.; Iijima, S. *Phys. Rev. Lett.* **2000**, *85*, 5384.
(4) Sloan, J.; Terrones, M.; Nufer, S.; Friedrichs, S.; Bailey, S. R.; Woo, H. G.; Ruhle, M.; Hutchison, J. L.; Green, M. L. H. *J. Am. Chem. Soc.* **2002**, *124*, 2116.
(5) Liu, C.; Fan, Y. Y.; Liu, M.; Cong, H. T.; Cheng, H. M.; Dresselhaus, M. S. *Science* **1999**, *286*, 1127.
(6) Tanaka, H.; El-Merraoui, M.; Steele, W. A.; Kaneko, K. *Chem. Phys. Lett.* **2002**, *352*, 334.
(7) Ajayan, P. M.; Ebbesen, T. W.; Ichihashi, T.; Iijima, S.; Tanigaki, K.; Hiura, H. *Nature* **1993**, *362*, 523.
(8) Murata, K.; Kaneko, K.; Steel, W. A.; Kokai, F.; Takahashi, K.; Kasuya, D.; Hirahara, K.; Yudasaka, M.; Iijima, S. *J. Phys. Chem. B* **2001**, *105*, 10210.
(9) Kiang, C. H.; Choi, J. S.; Tran, T. T.; Bacher, A. D. *J. Phys. Chem. B* **1999**, *103*, 7449.
(10) Hernadi, K.; Siska, A.; Thiên-Nga, L.; Forró L.; Kiricsi, I. *Solid State Ionics* **2001**, *141*−*142*, 203.
(11) Tsang, S. C.; Harris, P. J. F.; Green, M. L. H. *Nature* **1993**, *362*, 520.
(12) Kuznetsova, A.; Mawhinney, D. B.; Naumenko, V.; Yates, J. T., Jr.; Liu, J.; Smalley, R. E. *Chem. Phys. Lett.* **2000**, *321*, 292.
(13) Tsang, S. C.; Chen, Y. K.; Harris, P. J. F.; Green, M. L. H. *Nature* **1994**, *372*, 159.
(14) Raymundo-Piñero, E.; Cazorla-Amorós, D.; Linares-Solano, A.; Delpeux, S.; Frackowiak, E.; Szostak, K.; Béguin, F. *Carbon* **2002**, *40*, 1614.
(15) Chang, J. Y.; Ghule, A.; Chang, J. J.; Tzing, S. H.; Ling, Y. C. *Chem. Phys. Lett.* **2002**, *363*, 583.
(16) Yang, C. M.; Kaneko, K.; Yudasaka, M.; Iijima, S. *Nanoletters* **2001**, *1*, 487.
(17) Cinke, M.; Li, J.; Chen, B.; Cassell, A.; Delzeit, L.; Han, J.; Meyyappan, M. *Chem. Phys. Lett.* **2002**, *365*, 69.
(18) Iijima, S.; Yudasaka, M.; Yamada, R.; Bandow, S.; Suenaga, K.; Kokai, F.; Takahashi, K. *Chem. Phys. Lett.* **1999**, *309*, 165.
(19) Kasuya, D.; Yudasaka, M.; Takahashi, K.; Kokai, F.; Iijima, S. *J. Phys. Chem. B* **2002**, *106*, 4947.
(20) McKee, D. W. In *Chemistry and Physics of Carbon;* Walker, P. L., Thrower, P. A., Eds.; Marcel Dekker: New York, 1981; Vol. 16, p 54.
(21) Kuznetsova, A.; Popova, I.; Yates, J. T., Jr.; Bronikowski, M. J.; Huffman, C. B.; Liu, J.; Smalley, R. E.; Hwu, H. H.; Chen, J. G. *J. Am. Chem. Soc.* **2001**, *123*, 10699.
(22) Hu, H.; Bhowmik, P.; Zhao, B.; Hamon, M. A.; Itkis, M. E.; Haddon, R. C. *Chem. Phys. Lett.* **2001**, *345*, 25.
(23) Lee, W. H.; Kim, S. J.; Lee, W. J.; Lee, J. G.; Haddon, R. C.; Reucroft, P. J. *Appl. Surf. Sci.* **2001**, *181*, 121.
(24) Zielke, U.; Huttinger, K. J.; Hoffman, W. P. *Carbon* **1996**, *34*, 983.
(25) Ros, T. G.; van Dillen, A. J.; Geus, J. W.; Koningsberger, D. C. *Chem. Eur. J.* **2002**, *8*, 1151.
(26) Szymanski, G. S.; Karpinski, Z.; Biniak, S.; Swiatkowski, A. *Carbon* **2002**, *40*, 2627.
(27) Murata, K.; Kaneko, K.; Steele, W. A.; Kokai, F.; Takahashi, K.; Kasuya, D.; Hirahara, K.; Yudasaka, M.; Iijima, S. *J. Phys. Chem. B* **2001**, *105*, 10210.
(28) Setoyama, N.; Suzuki, T.; Kaneko, K. *Carbon* **1998**, *36*, 1459.
(29) Bekyarova, E.; Kaneko, K.; Kasuya, D.; Murata, K.; Yudasaka, M.; Iijima, S. *Langmuir* **2002**, *18*, 4138.
(30) Nagasawa, S.; Yudasaka, M.; Hirahara, K.; Ichihashi, T.; Iijima, S. *Chem. Phys. Lett.* **2000**, *328*, 374.
(31) Borowiak-Palen, E.; Pichler, T.; Liu, X.; Knupfer, M.; Graff, A.; Jost, O.; Pompe, W.; Kalenczuk, R. J.; Fink, J. *Chem. Phys. Lett.* **2002**, *363*, 567.
(32) Nikolaev, P.; Tess, A.; Rinzler, A. G.; Colbert, D. T.; Smalley, R. E. *Chem. Phys. Lett.* **1997**, *266*, 422.
(33) Terrones, M.; Terrones, H.; Banhart, F.; Charlier, J.-C.; Ajayan, P. M. *Science* **2000**, 288, 1226.
(34) Bekyarova, E.; Hanzawa, Y.; Kaneko, K.; Silvestre-Albero, J.; Sepulveda-Escribano, A.; Rodriguez-Reinoso, F.; Kasuya, D.; Yudasaka, M.; Iijima, S. *Chem. Phys. Lett.* **2002**, *366*, 463.
(35) Hamon, M. A.; Chen. J.; Hu, H.; Chen, Y.; Itkis, M. E.; Rao, A. M.; Eklund, P. C.; Haddon, R. C. *Adv. Mater.* **1999**, *11*, 834.
(36) Rodriguez-Reinoso, F.; Pastor, A. C.; Marsh, H.; Huidobro, A. *Carbon* **2000**, *38*, 397.
(37) Figueiredo, J. L.; Pereira, M. F. R.; Frietas, M. M. A.; Orfao, J. J. M. *Carbon* **1999**, *37*, 1379.
(38) Marchon, B.; Carrazza, J.; Heinemann, H.; Somorjai, G. A. *Carbon* **1988**, *26*, 507.
(39) Takhagi, T.; Ishitani, I. *Carbon* **1984**, *22*, 43.
(40) Haydar, S.; Moreno-Castilla, C.; Ferro-Garcia, M. A.; Carrasco-Martin, F.; Rivera-Utrilla, J.; Perrard, A.; Joly, J. P. *Carbon* **2000**, *38*, 1297.